

# Solid renal masses in adults

**Maresh Kumar Mittal, Binit Sureka<sup>1</sup>**

Department of Radiodiagnosis, Vardhman Mahavir Medical College and Safdarjung Hospital, <sup>1</sup>Department of Radiology, Institute of Liver and Biliary Sciences, New Delhi, India

**Correspondence:** Dr. Binit Sureka, Department of Radiology, Institute of Liver and Biliary Sciences, New Delhi - 110 070, India.  
E-mail: binitSUREKAPGI@gmail.com

## Abstract

With the ever increasing trend of using cross-section imaging in today's era, incidental detection of small solid renal masses has dramatically multiplied. Coincidentally, the number of asymptomatic benign lesions being detected has also increased. The role of radiologists is not only to identify these lesions, but also go a one step further and accurately characterize various renal masses. Earlier detection of small renal cell carcinomas means identifying at the initial stage which has an impact on prognosis, patient management and healthcare costs. In this review article we share our experience with the typical and atypical solid renal masses encountered in adults in routine daily practice.

**Key words:** Adults; renal masses; RCC; solid

## Introduction

The diagnosis of renal masses has increased in the last decades owing to the widespread use of computed tomography (CT) and magnetic resonance imaging (MRI). Renal cell carcinoma (RCC) accounts for 3% of all adult cancer and 85% of all kidney tumors.<sup>[1]</sup> Based on the data from developed countries, RCC is considered to be the malignancy of 6–7<sup>th</sup> decade of life, however, data from India shows that it affects at a younger age.<sup>[2]</sup> Benign tumors account for 15–20% of all solid renal cortical tumors, and renal oncocytoma is the most common solid tumor type.<sup>[3]</sup>

Renal masses are divided into solid, cystic, and complex cystic lesions. On imaging, 85% of expansive bean-type solid masses are malignant.<sup>[4]</sup> Therefore, a solid, enhancing mass must be considered malignant unless proven otherwise. Moreover, one should be aware of less common neoplasms such as mesenchymal renal tumors and various renal pseudotumors that can be seen on imaging.

## Imaging

Majority of the renal masses are detected incidentally on routine ultrasound examination. Fortunately, most of these lesions are simple cortical cysts and do not require further radiological investigation. Ultrasound, as a diagnostic tool, is helpful to triage renal lesions which will require further imaging workup. It is useful in distinguishing cysts from hypovascular solid tumors seen on CT and it also reveals septations better in cases of complex cystic lesions. Ultrasound is also useful for assessing the presence and extent of venous thrombus by the application of Doppler. Recently, contrast-enhanced ultrasound (CEU) has also shown promising results in differentiating various subtypes of RCC and benign lesions such as angiomyolipomas (AML) and oncocytomas.<sup>[5,6]</sup> The major advantage is that it can be safely used in patients with renal insufficiency.<sup>[7]</sup> The role of PET in renal masses is in staging, detection of metastases, and for follow-up.<sup>[8]</sup> Solid and complex cystic masses detected on ultrasound require further imaging evaluation with CT and/or MRI for proper characterization.

### Access this article online

#### Quick Response Code:



**Website:**  
www.ijri.org

**DOI:**  
10.4103/0971-3026.195773

This is an open access article distributed under the terms of the Creative Commons Attribution-NonCommercial-ShareAlike 3.0 License, which allows others to remix, tweak, and build upon the work non-commercially, as long as the author is credited and the new creations are licensed under the identical terms.

**For reprints contact:** reprints@medknow.com

**Cite this article as:** Mittal MK, Sureka B. Solid renal masses in adults. Indian J Radiol Imaging 2016;26:429-42.

Four phase, i.e., unenhanced, corticomedullary (20–40 seconds), nephrographic (80–90 seconds) and excretory phase (180–300 seconds) contrast-enhanced CT scan is recommended for detailed evaluation and characterization of renal masses. Unenhanced images of the kidneys allow the detection of calcification or fat. On contrast-enhanced CT, enhancement is considered significant if it is more than +15HU. If the enhancement is between 10–15 HU, the mass is indeterminate. Tumors that do not meet the criteria of a typical carcinoma or AML are said to be indeterminate.<sup>[9]</sup> Dual energy multiple detector (MDCT) is a promising recent advancement for imaging in renal masses particularly in cases where renal protocol has not been followed and in renal cysts showing pseudoenhancement.<sup>[10]</sup> Dual-energy CT (DECT) is being increasingly used for the characterization of renal masses because of its incremental benefit of material characterization without significant increase in radiation dose. The ability to selectively identify iodine containing image voxels from contrast-enhanced dual-energy scans using material decomposition algorithm has enabled characterization of renal lesions from single contrast-enhanced phase of examination without the need for an unenhanced phase.<sup>[11]</sup> This is especially helpful in characterizing incidentally detected renal lesions, which could avoid the need for repeat imaging with a dedicated renal mass protocol, thus saving radiation dose to the patient and the need for repeat contrast administration. Moreover, the degree of enhancement can be quantified by measuring the density of iodine density within the lesions. Using dual-source DECT, an iodine density threshold of 0.5 mg/mL has been reported to have sensitivity and specificity of 100% and 97.7% for distinguishing enhancing from non-enhancing lesions.<sup>[12]</sup> Tumor iodine concentration of 0.9 mg/mL has been reported to represent an optimal threshold to discriminate between clear cell and papillary renal cell cancers.<sup>[13]</sup>

MRI is used when optimal CT cannot be performed, as in the case of a severe allergy to iodinated contrast medium or pregnancy. MRI may serve as a useful tool for the characterization of renal masses because few of the renal masses can have distinct features at MR imaging, which will be discussed in relevant sections.<sup>[14]</sup> Renal masses with borderline enhancement on CT should be further evaluated with MRI or contrast-enhanced ultrasound. The role of diffusion-weighted MRI as a biomarker for evaluation of benign and malignant renal tumors, different subtypes of RCC, and histological grades is under evaluation.<sup>[15]</sup>

### The Ball versus the Bean

In 2006, David S. Hartman and Pablo R. Ros from the Armed Forces Institute of Pathology designed a strategy for the evaluation of renal masses and developed a concept known

as ball-type or bean-type renal masses depending upon the growth pattern.<sup>[16-18]</sup>

The ball-type renal masses are more common. The ball-type lesion typically deforms the renal contour, producing a hump or contour bulge. Collecting system elements are displaced. These masses are better seen on nephrographic phase because they are more conspicuous against the background of normally enhancing renal parenchyma. The bean-type lesions use the renal tissue as scaffolding for their growth, thus causing enlargement of the kidney, while maintaining its reniform (bean) shape. The bean-type masses are invisible on unenhanced images and are best appreciated on nephrographic and excretory phase images. Collecting system elements are destroyed by the bean-type masses [Figure 1].<sup>[16]</sup> The list of ball and bean type renal masses is detailed in Table 1.

### Renal Cell Carcinoma

RCC is the eighth most common malignancy affecting the adults; the seventh most common cancer in men and the ninth most common in women.<sup>[19,20]</sup> RCC is the most common tumor to involve the kidneys and accounts for 80–90% of primary malignant renal neoplasms in adults. According to the latest 2004 World Health Organisation (WHO) classification, RCC is classified into various subtypes, as detailed in Table 2.<sup>[21]</sup>

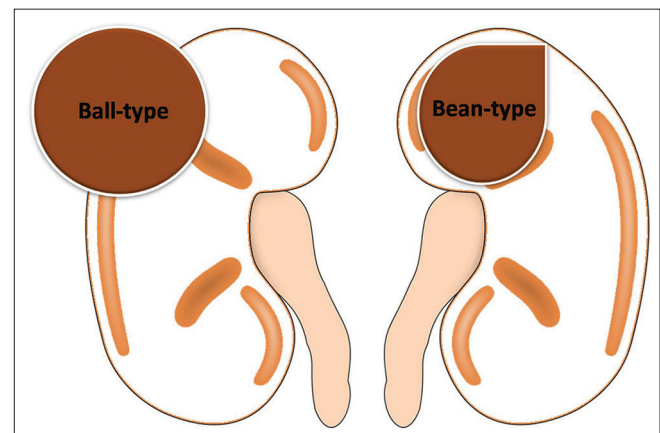


**Figure 1:** Line diagram showing ball and bean-type renal mass

**Table 1: Ball and Bean type renal masses<sup>[16]</sup>**

| Type of renal mass | Pathology  |
|--------------------|--|
| Ball-type lesions  | Renal cell carcinoma<br>Angiomyolipoma<br>Oncocytoma<br>Metastasis<br>Lymphoma   |
| Bean-type lesions  | Transitional cell carcinoma<br>Infiltrative renal cell carcinoma<br>Medullary carcinoma<br>Collecting duct carcinoma<br>Metastasis |

**Clear cell RCC** – This is the most common (80%) subtype of RCC. Most clear cell RCCs are solitary but multicentricity (4%) and bilaterality (0.5–3%) may also be seen. On imaging, clear cell carcinoma is typically highly vascular. Necrosis, cystic degeneration, hemorrhage, calcification, and ossification may occur [Figures 2-8].<sup>[22,23]</sup> Clear cell RCC has a worse prognosis when compared with chromophobe or papillary subtypes. The MR imaging features of clear cell type RCC varies depending on the presence of cystic, hemorrhage, and necrotic components. Loss of signal intensity within the solid portions of clear cell RCCs on opposed phase images is due to cytoplasmic fat and has been observed in up to 60% of these tumors.<sup>[24]</sup>

**Papillary RCC** – Papillary subtype accounts for 15% of RCC.<sup>[19]</sup> Papillary tumors are divided into two subtypes. Type I occurs sporadically and metastasizes somewhat

**Table 2: Renal cell carcinoma subtypes**

|   |
|---|
| Clear cell renal cell carcinoma                             |
| Multilocular clear cell renal cell carcinoma                |
| Papillary renal cell carcinoma                              |
| Chromophobe renal cell carcinoma                            |
| Carcinoma of the collecting ducts of Bellini                |
| Renal medullary carcinoma                                   |
| Xp11 translocation carcinomas                               |
| Carcinoma associated with neuroblastoma                     |
| Mucinous tubular and spindle cell carcinoma <sup>[21]</sup> |
| Renal cell carcinoma unclassified                           |

later whereas Type II variety is inherited, may be multiple, and often presents with a higher histological grade.<sup>[19]</sup> On imaging, papillary RCCs are hypovascular [Figure 9]. Various studies have shown that tumor-to-aorta and tumor-to-kidney ratios in the arterial and delayed phases are lower in papillary subtype. Herts *et al.* suggested that the strongest predictor of a papillary RCC was a tumor-to-kidney attenuation ratio of less than 0.25 in the arterial phase and the excretory phase.<sup>[25]</sup> Papillary RCCs appear as well-encapsulated masses with homogeneous low signal intensity on T2-weighted images and homogeneous low-level enhancement after the intravenous administration of contrast material, or as cystic hemorrhagic masses with peripheral enhancing papillary projections.<sup>[24]</sup>

**Chromophobe RCC** – This subtype accounts for 5% of RCC and has the best prognosis. The tumor cells arise from the cortical collecting duct epithelium. Calcification is more common in this subtype according to a previous study.<sup>[26]</sup> On imaging, these tumors are hypovascular and show homogeneous enhancement may show central scar or necrosis [Figure 10]. The enhancement characteristics fall in between those of clear cell and papillary RCC.<sup>[7]</sup> Raman *et al.* in their study showed that the tumor-to-cortex ratios

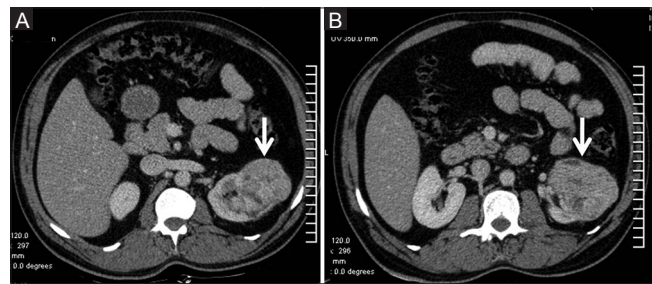


**Figure 2 (A and B):** (A and B) Clear cell RCC: Contrast-enhanced CT showing typical features of clear cell RCC –ball type lesion causing smooth contour bulge, showing heterogeneous enhancement with areas of necrosis within the tumor

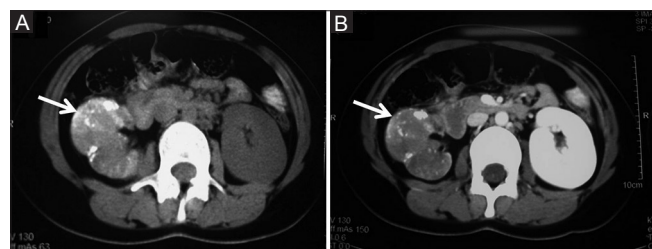


**Figure 4 (A and B):** (A, B) Clear cell RCC with calcification: Axial contrast-enhanced CT images showing heterogeneously enhancing ball type lesion in right kidney with specks of calcification within the tumor

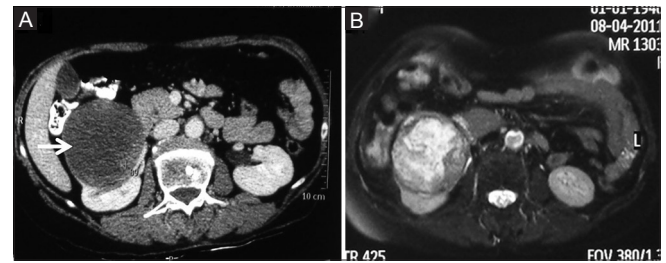


**Figure 3 (A and B):** Necrotic RCC: (A) Contrast-enhanced CT image showing a predominantly necrotic mass in right kidney (B) Axial T2-weighted MR images showing T2 hyperintense necrotic centre with solid component within the tumor

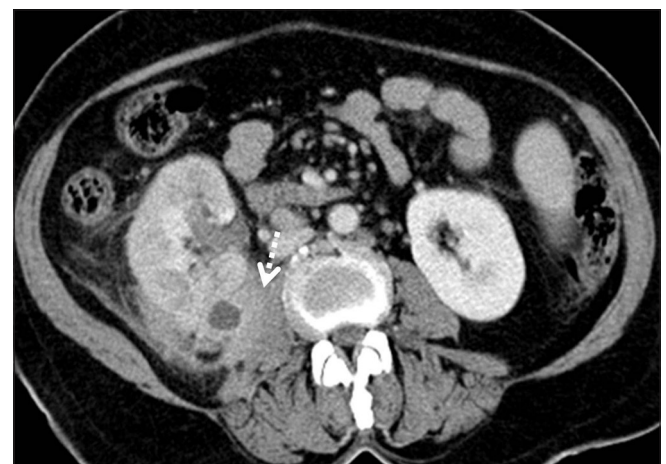


**Figure 5:** Clear cell RCC with paraspinal invasion: Axial contrast-enhanced CT image showing right RCC with extension and invasion into the right paraspinal muscle (dashed arrow)

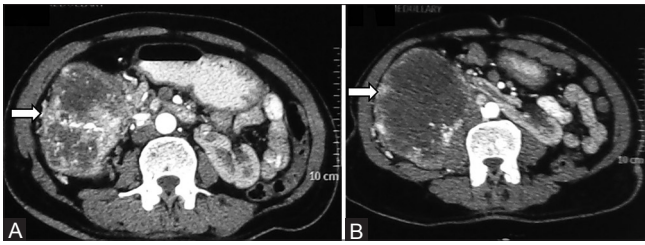


**Figure 6 (A and B):** (A, B) Clear cell RCC in horseshoe kidney: Axial contrast-enhanced CT image showing horseshoe kidneys with a heterogeneously enhancing clear cell RCC in right moiety

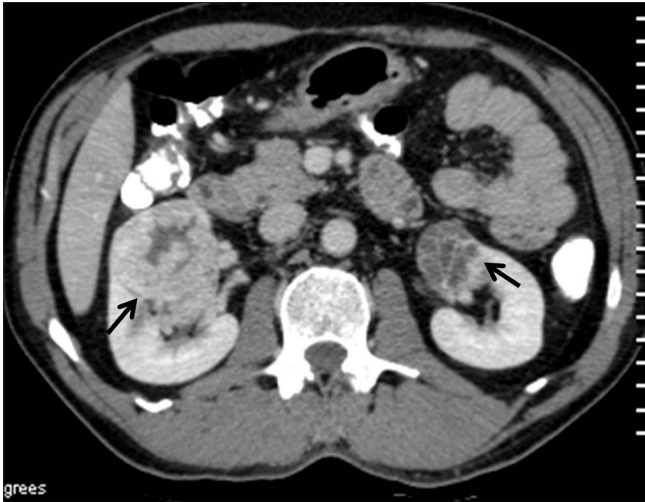


**Figure 8:** Bilateral RCC: Axial contrast-enhanced CT image showing heterogeneously enhancing renal masses in both the kidneys proven to be bilateral RCCs

for chromophobe RCCs were 0.59, 0.48, and 0.50 in the corticomedullary, nephrographic, and excretory phases, respectively.<sup>[27]</sup>

*Carcinoma of the collecting ducts (CDC) of Bellini* – This subtype accounts for <1% of RCC.<sup>[28]</sup> Mean patient age is 55 years with a slight male predominance. On imaging, medullary location, weak, and heterogeneous enhancement, infiltrative pattern of growth is identified.<sup>[28]</sup>

*Renal medullary carcinoma* –It is a rapidly growing, aggressive subtype of RCC seen in young male blacks of African ethnicity with sickle cell trait. It has also been described as an aggressive variant of CDC. Metastasis may be evident at the initial presentation and the prognosis is poor [Figure 11].<sup>[4]</sup> Notably, this tumor mostly develops on the right side of the body.<sup>[29]</sup> On imaging, this tumor presents as an infiltrative necrotic renal mass, with caliectasis and regional lymphadenopathy, usually on the right side.<sup>[30]</sup>

*Renal carcinoma associated with Xp11.2 translocations/TFE3 gene fusions* –This carcinoma predominantly affects children and young adults. On histopathological examination, it mimics like a papillary carcinoma with clear cells and cells with granular eosinophilic cytoplasm. On imaging, large

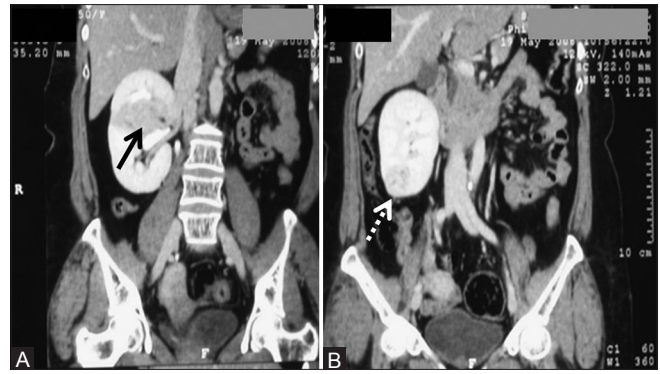


**Figure 7 (A and B):** (A, B) Multifocal RCC: Coronal CECT images showing two RCCs – one in interpolar region (arrow) and another in lower pole (dashed arrows) in right kidney

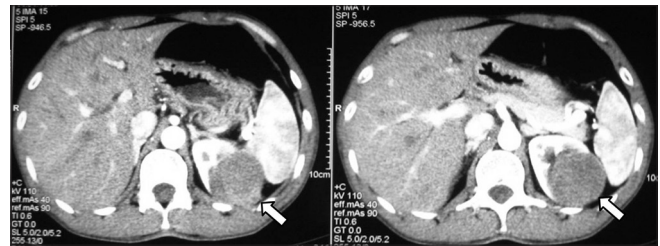


**Figure 9:** Papillary RCC: Axial contrast-enhanced CT images showing hypovascular bean-type left renal mass proven to be papillary RCC

size, cystic changes, calcification, high-attenuating areas on unenhanced scans, aggressive behaviour of lymph node, and distant metastasis favor this subtype of RCC, especially in a young female patient.<sup>[31,32]</sup>

*Multilocular cystic renal cell carcinoma (MCRCC)* –This tumor has an excellent prognosis. It has a male predominance seen in 2–7<sup>th</sup> decade of life. On imaging, it is entirely composed of cysts of variable size separated from the kidney by a fibrous capsule [Figures 12 and 13]. The imaging spectrum may range from Bosniak IIF to Bosniak IV cystic lesion. However, the most common imaging appearance is Bosniak III complex cystic lesion. They cannot be distinguished from other complex cystic renal lesions by imaging. Their final diagnosis is made by histopathological analysis after surgical resection. The differential diagnosis of MCRCC is cystic nephroma, cystic clear cell RCC, clear cell variant of papillary RCC, cystic necrosis in RCC, and tubulocystic carcinoma.<sup>[33]</sup>

## Oncocytoma

Oncocytoma is a benign renal epithelial neoplasm derived from intercalated cells. It is the most common, benign, solid, nonfat-containing renal mass. It accounts for approximately 3–7% of all renal cortical neoplasms. Three pathological subtypes are seen, namely, organoid, tubulocystic, and mixed pattern.<sup>[34]</sup> Typical imaging findings of renal oncocytoma are homogeneous hypervascular mass with subsequent washout in the delayed phase with

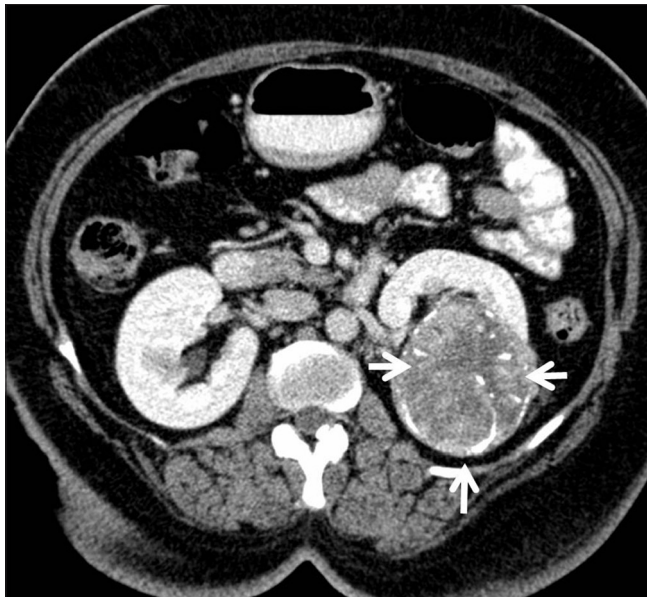


**Figure 10:** Chromophobe RCC: Axial contrast-enhanced CT image showing ball-type left renal mass with spoke-wheel enhancement histopathologically confirmed chromophobe RCC



**Figure 12:** Multicystic RCC: Coronal contrast-enhanced CT image showing multicystic upper pole right renal mass with thick enhancing septae and irregular walls suggestive of Bosniak IV cyst, histopathologically proved to be multicystic RCC

or without a central scar. A central scar is a characteristic finding, especially in a large oncocytoma [Figure 14]. In many cases, renal oncocytomas cannot be accurately distinguished RCC.<sup>[35]</sup>

Various enhancement patterns have been described in renal oncocytomas. Kim *et al.*<sup>[36]</sup> have postulated that segmental enhancement inversion on the corticomedullary

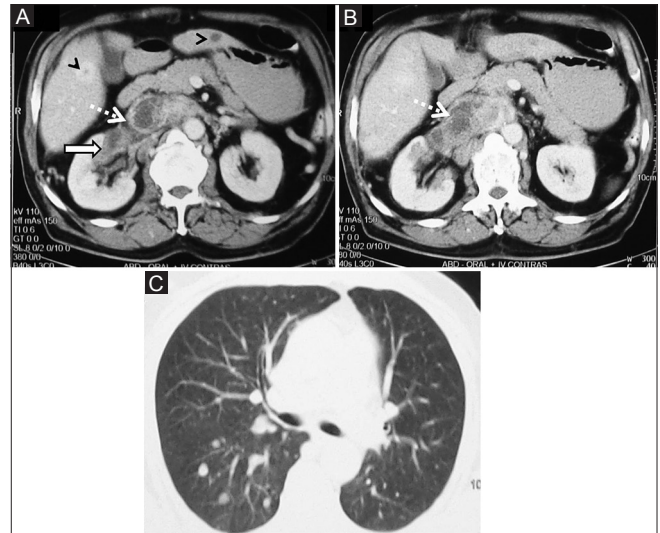


**Figure 11 (A-C):** Medullary RCC:(A, B) Axial contrast-enhanced CT abdomen images showing bean-type right renal mass centrally located (arrow) with right renal vein and IVC tumoral thrombus (dashed arrow) with liver metastases (arrowhead) (C) CT lung section showing pulmonary metastases

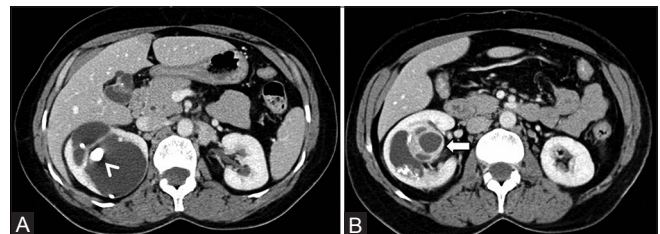


**Figure 13 (A and B):** Cystic RCC with calcification (A, B): Axial contrast-enhanced CT image showing predominantly cystic lesion with enhancing solid component (arrow) and calcification (arrowhead)

and early excretory phase is a characteristic enhancement pattern in small (<4cm) oncocytoma. Segmental enhancement inversion is defined as two distinct zones of enhancement, which show inverse patterns between the corticomedullary (30–40 s) and early excretory (120–180 s) phases in which one zone is hyperenhancing on the corticomedullary phase, which subsequently becomes hypoenhancing on the early excretory phase. The other zone is hypoenhancing on the corticomedullary phase and becomes hyperenhancing on the early excretory phase [Figure 15]. McGahan *et al.*<sup>[37]</sup> described that the most common feature of small oncocytoma (<4 cm) is a heterogeneous enhancing mass that becomes homogeneous on the delayed phase.

Cystic change and haemorrhage in renal oncocytomas ranges 5-20%.<sup>[38]</sup> Calcification is uncommon, but when present, may be seen within the central scar. Rarely, oncocytomas can present as a multilocular cystic mass. Telangiectatic variant has also been described, which is histologically characterized by multicystic spaces filled with blood products.<sup>[39]</sup>

Coexisting RCC is not rare in patients with oncocytoma with a reported incidence up to 10%.<sup>[40]</sup> Coexisting RCC may present as an incidental microscopic finding as a hybrid tumor or as a separate mass in the ipsilateral or contralateral kidney. Hybrid tumors consisting of oncocytoma and chromophobe RCC components have also been described in the literature and the differentiation is extremely difficult on imaging. Oncocytomas are multifocal in 2.5–16% of cases and bilateral in 4–12%.<sup>[41]</sup> Multifocal oncocytomas can be either sporadic or syndromic as seen in Birt–Hogg–Dube syndrome and tuberous sclerosis. Renal oncocytosis is a recently established disease entity defined as diffuse replacement of the renal parenchyma by numerous oncocytic tumors, such as hybrid tumors, chromophobe RCCs, renal oncocytomas, and oncocytic renal parenchyma.<sup>[35,42]</sup>

Oncocytoma has a variable and nonspecific appearance on MRI. The central scar if present shows low signal intensity on T1-weighted images and high signal intensity on T2-weighted images with delayed enhancement.<sup>[14,43]</sup> Sun *et al.*<sup>[44]</sup> in their series of 152 patients with solid renal masses concluded that all masses found to contain macroscopic fat with or without hemorrhage were considered to be benign. The remaining masses (without macroscopic fat) found not to contain hemorrhage were considered to be benign. Only those found to contain hemorrhage alone were considered to be malignant. By combining the results for the macroscopic fat and hemorrhage, the accuracy, sensitivity, and specificity in the differential diagnosis of the benign and malignant masses in their study was 96.05%, 95.19%, and 97.92%, respectively. Davarpanah *et al.*<sup>[45]</sup> concluded that homogeneous T1 hyperintense renal lesion with a smooth border and signal intensity of at least 2.5 times higher than the surrounding renal parenchyma has a greater than 99.9% chance of representing a benign hemorrhagic or proteinaceous cyst. Familial syndromes and their association with different types of renal masses are enlisted in Table 3.



**Figure 14:** Oncocytoma with central scar: Axial contrast-enhanced CT image showing large left renal mass with central scar (arrowhead) histopathologically proven giant oncocytoma

## Lymphoma

Renal lymphoma has a variable imaging spectrum and may mimic RCC. Lymphomatous involvement of kidneys may be classified as primary renal lymphoma (PRL) and secondary renal lymphoma (SRL). Secondary lymphomatous renal involvement is more common. PRL is exceedingly rare, accounting for less than 1% of extranodal lymphomas.<sup>[46]</sup> PRL should be diagnosed only in the following situations: disease localized to the kidney, presentation with renal failure in the absence of other causes of renal impairment, rapid improvement of renal function after treatment of lymphoma, or diagnosis confirmed by biopsy.<sup>[47]</sup> Most common type is nonHodgkin lymphoma, usually the B-cell type.

On imaging, renal lymphoma has a wide variety of manifestations – solitary or multiple lesions, direct extension from retroperitoneal adenopathy, preferential involvement of the perinephric space, and diffuse infiltration of one or both kidneys [Figures 16-19]. Lymphomatous deposits enhance less than the normal renal tissue and appear as relatively homogeneous masses with lower attenuation than that of the surrounding cortex.<sup>[48]</sup> Rarely, PRL can

**Table 3: Familial syndromes associated with renal masses<sup>[23]</sup>**

| Syndrome                                  | Renal mass                                 |
|---|--|
| Von Hippel-Lindau (VHL)                   | Clear cell RCC                             |
| Tuberous Sclerosis                        | Angiomyolipoma, clear cell RCC, oncocytoma |
| Familial renal carcinoma                  | Clear cell RCC                             |
| Hereditary Papillary RCC                  | Papillary RCC                              |
| Familial oncocytoma                       | Oncocytoma                                 |
| Hereditary leiomyoma-RCC                  | Papillary RCC                              |
| Birt-Hogg-Dube (BHD)                      | Chromophobe RCC, oncocytoma, hybrid tumors |
| Constitutional chromosome 3 translocation | Clear cell RCC                             |



**Figure 15 (A and B):** (A, B) Oncocytoma with segmental enhancement inversion: Coronal contrast-enhanced MR images (A) small ball-type renal mass in lower pole of right kidney showing peripheral enhancement in corticomedullary phase and (B) central enhancement in excretory phase suggestive of oncocytoma



**Figure 16:** Infiltrative lymphoma: Axial contrast-enhancedCT image showing bilateral enlarged hypodense kidneys (arrow) giving the appearance of bean-type renal mass with enlarged retroperitoneal lymph nodes

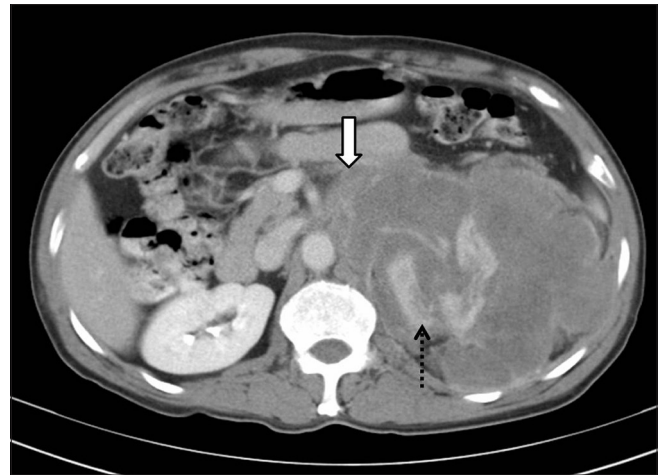


**Figure 17:** Lymphoma –Direct extension from retroperitoneum: Axial contrast-enhancedCT image showing retroperitoneal lymphadenopathy (arrow) infiltrating the left kidney (dashed arrow)



**Figure 18:** Perinephric lymphoma: Axial contrast-enhancedCT image showing hypodense perinephric soft tissue surrounding the left kidney in a case of perinephric lymphoma

present as a mass predominantly involving the renal sinus. PRL rarely invade the renal vein and inferior vena cava differentiating it from RCC. On MRI, lymphomatous masses are usually hypointense relative to the renal cortex on T2-weighted images and enhance minimally on delayed gadolinium-enhanced images.<sup>[6]</sup> Hematoma, sarcoma, extramedullary hematopoiesis, and metastases are the main differential diagnoses for perinephric masses. Infection, leukemia, collecting duct, or medullary carcinoma may present with bilateral nephromegaly.<sup>[49]</sup>

### Angiomyolipoma

AML is the most common benign solid renal neoplasm observed in clinical practice and belongs to the family of newly classified tumours known as perivascular epithelioid cell differentiation also known as “PEComa.” Radiologically,



**Figure 19:** Solitary mass forming lymphoma: Axial contrast-enhancedCT image showing solitary hypoenhancing lesion in left kidney histopathologically confirmed lymphoma

AMLs are classified into sporadic or syndromic. In sporadic variety, various subtypes such as triphasic, classic, fat poor AML, hyperattenuating AML, isoattenuating AML, AML with epithelial cysts, and epithelioid AML are seen. Syndromic AMLs are seen in tuberous sclerosis and lymphangioleiomyomatosis.<sup>[50]</sup>

*Triphasic AML* –It occurs sporadically in less than 0.2% of the population with a female predilection in the 4–6<sup>th</sup> decade of life. It is a benign mesenchymal tumor composed of dysmorphic blood vessels, smooth muscle components, and mature adipose tissue. Triphasic AML is further subdivided radiologically into classic and fat poor subtypes.<sup>[51]</sup> Classical AML is characterized by the presence of fat. On ultrasound, classic AML is hyperechoic due to the presence of fat. The presence of anechoic rim, intratumoral cysts, or acoustic shadowing can be present in both AML and RCC, and therefore, this modality cannot reliably differentiate both.<sup>[52,53]</sup> On CT and MRI, presence of fat is diagnostic [Figure 20].

Intratumoral hemorrhage may occur, particularly in tumors larger than 4 cm, and make the diagnosis of AML confusing and may mimic a RCC. The presence of enlarged or bridging vessels, aneurysms, and perinephric hematomas are additional imaging features of AML. Calcification is uncommon in AML.<sup>[54]</sup> Fat poor AML are also known as “AML with minimal fat” or “lipid-poor AML.” Fat poor AMLs are divided into three subtypes—hyperattenuating, isoattenuating AML, and AML with epithelial cysts. Hyperattenuating AML represent approximately 4–5% of all AML.<sup>[55]</sup> They are typically small than 3 cm in diameter. On imaging, these lesions are homogeneously isoechoic on ultrasound, hyperattenuating (>45 HU) on unenhanced CT, and hypointense on T1 and T2-weighted MRI. Post contrast, these lesions show homogeneous enhancement. The differentials of a hyperattenuating renal mass are RCC, hyperattenuating AML, and oncocytoma. Isoattenuating AMLs show attenuation of –10 to 45 HU on unenhanced CT and have homogeneous delayed enhancement. Although there is no characteristic imaging feature, a homogeneously enhancing renal mass that is both T2-hypointense and suppresses on chemical shift imaging should prompt consideration of an isoattenuating AML.

*AML with epithelial cysts* – These lesions are more common in women and contain very little fat. On imaging, solid-cystic lesion is seen where the solid component shows enhancement pattern similar to fat poor AML. The differentials to be considered are multilocular cystic RCC, multilocular cyst, cystic nephroma, and a mixed epithelial and stromal tumor (MEST).<sup>[56]</sup>

*Epithelioid AML* – Epithelioid AML is an extremely rare subtype of AML misdiagnosed as sarcomatoid or high grade RCC. Unlike all other AMLs, the epithelioid type is potentially malignant, aggressive and can metastasize.<sup>[57,58]</sup> Radiologically, epithelioid AMLs typically present as large masses, solid-cystic or multicystic mass with intratumoral hemorrhage and necrosis.

*AML in tuberous sclerosis and lymphangioliomyomatosis* – AMLs are observed in 55–75% of patients with TSC;<sup>[59]</sup> most form by the third decade. AMLs in tuberous sclerosis typically present at a younger age, are multiple, larger, tend

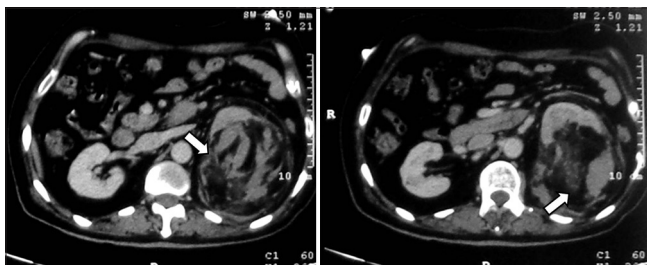


**Figure 20:** Triphasic angiomyolipoma: Axial contrast-enhanced CT images showing ball-type left renal mass with fat, blood vessel, and soft tissue component

to bleed, and almost always bilateral [Figure 21].<sup>[59]</sup> AMLs in lymphangioliomyomatosis are typically smaller, less frequently bilateral, and less prone to bleeding than those found in patients with tuberous sclerosis.<sup>[60]</sup>

## Renal Metastases

The kidney is a rare site of metastasis. The reported incidence of renal metastasis of extrarenal neoplasms varies 2–20%.<sup>[61,62]</sup> Metastatic renal disease is seldom clinically identified because the symptoms of pain and hematuria occur in only 20% of patients. Excluding lymphoma, the most common primary tumor that metastasizes to the kidney is lung carcinoma. Metastases from a primary tumor treated previously may mimic renal tumors. On imaging, CT is the most accurate method to screen for secondary renal tumors. But the appearance of renal metastasis on CT may be mimicked by RCC, transitional cell carcinoma, pyelonephritis, or phlegmon. On imaging, metastases are commonly small, multicentric, and bilateral, but less than 2% of renal cell carcinomas may also display this imaging pattern [Figures 22 and 23].<sup>[62]</sup>

## Infiltrative Renal Cell Carcinoma and Transitional Cell Carcinoma

Radiologically, intrarenal transitional cell carcinoma (TCC) presents as a centrally invasive renal mass, also referred to as “centrally infiltrating” or “intrarenal” TCC. It was first described as a renal pelvic carcinoma in 1841 by French pathologist Rayer.<sup>[63]</sup> Intrarenal TCC is a close radiologic mimic of other infiltrative renal masses, especially centrally located RCC. Imaging differentiation of these two entities is difficult because management strategies differ. Centrally located RCC is surgically treated with nephrectomy, whereas intrarenal TCC requires nephroureterectomy and often wider lymphadenectomy.<sup>[64]</sup>

On imaging, features suggestive of intrarenal TCC are filling defect in the renal pelvis, irregular, narrowed or amputated collecting system, circumferential urothelial thickening, tumor epicentre within the collecting system,

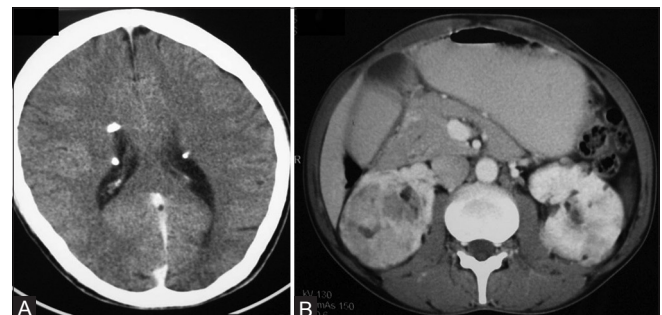


**Figure 21 (A and B):** AML in Tuberous sclerosis: (A) CT head image showing calcified subependymal nodules (B) contrast-enhanced CT abdomen image showing multiple fat-containing lesions in bilateral kidneys suggestive of AMLs



renal shape preservation, absence of cystic or necrotic change, homogeneity of the tumor, and extension into the ureteropelvic junction [Figures 24-26].<sup>[65,66]</sup> On MRI, TCC may be seen as an irregular, enhancing filling defect in the pelvicaliceal system or ureter.<sup>[6]</sup>

## Mesenchymal Neoplasms

Mesenchymal neoplasms in the kidneys can be benign or malignant. Benign mesenchymal neoplasms include AML, leiomyoma, hemangioma, lymphangioma, juxtaglomerular cell tumor, medullary fibroma, lipoma, solitary fibrous tumor, and schwannoma. Malignant neoplasms are sarcomas (leiomyosarcoma, rhabdomyosarcoma, angiosarcoma, osteosarcoma, synovial sarcoma, fibrosarcoma), and malignant fibrous histiocytoma.<sup>[25,67]</sup>

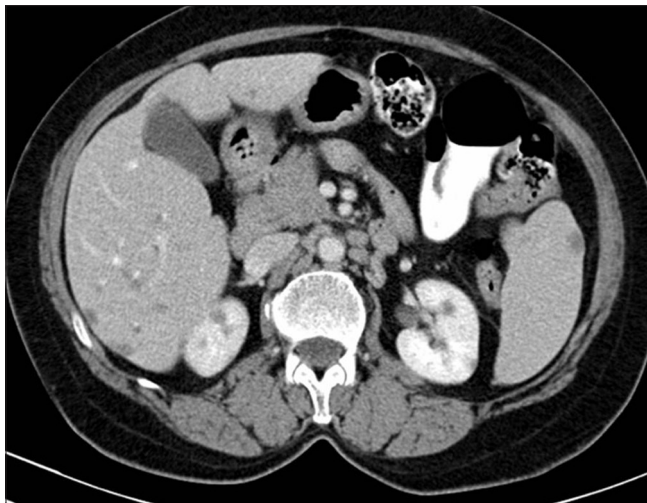


**Figure 22:** Renal metastases: Axial contrast-enhanced CT image showing hypodense multiple metastases in liver, kidneys, and spleen in a known case of carcinoma rectum

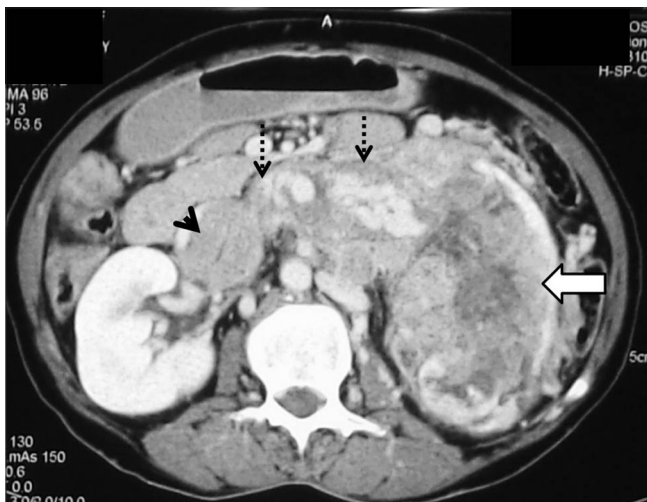


**Figure 24:** Infiltrative RCC: Axial contrast-enhanced CT image showing heterogeneously enhancing infiltrative RCC (arrow) in left kidney giving a bean-type appearance with enhancing tumor thrombus in left renal vein (dashed arrow), and IVC (arrowhead)

Most characteristic imaging feature is of AML, which has been described separately. Other mesenchymal neoplasms are difficult to accurately diagnose on imaging preoperatively. However, certain imaging features such as presence of fatty component (AML, lipoma), cystic component (lymphangioma), and calcified component (hemangioma, osteosarcoma) may be a clue to the diagnosis [Figures 27-30].

## Mixed Mesenchymal and Epithelial Tumors

Cystic nephroma, mixed epithelial, and stromal tumor belong to this category of renal neoplasms. Multicystic nephroma (MCN) is a rare benign cystic lesion of the kidney. It has a bimodal age distribution, occurring in both infants and adult population. Although it has been described in neonates, MCN is more commonly seen in the age group of 2–4 years; with a male to female ratio is 3:1.<sup>[68]</sup> In adults, it is seen in the 4–6<sup>th</sup> decade and more common in females. Unilateral involvement is more common and the lower pole of kidney is affected usually. CT imaging features of MCN are multicystic architecture, noncommunicating cysts with well-defined margins, enhancing septae, and herniation into renal pelvis [Figure 31]. Central or small peripheral curvilinear calcifications can occasionally be seen.<sup>[69]</sup> On MRI, imaging features include hypointense signal on T1-weighted sequences and hyperintense signal on T2-weighted sequences suggesting cystic nature. The most important differential diagnosis is multicystic RCC.

## Renal Pseudotumors

Renal pseudotumors are lesions which mimic renal cell carcinoma. Such masses are composed of normal or

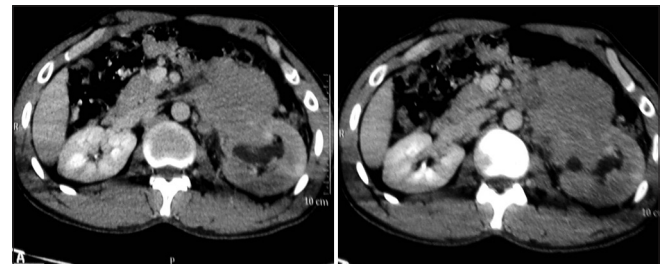


**Figure 23:** Renal metastases: Axial contrast-enhanced CT images showing retroperitoneal lymphadenopathy infiltrating into left kidney in a known case of metastases from testicular malignancy

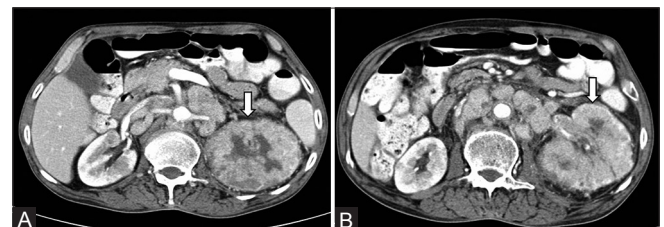


**Figure 25 (A and B):** (A, B) Infiltrative RCC: Axial CECT images showing expansive bean-type renal mass involving the left kidney (arrow) with retroperitoneal lymphadenopathy

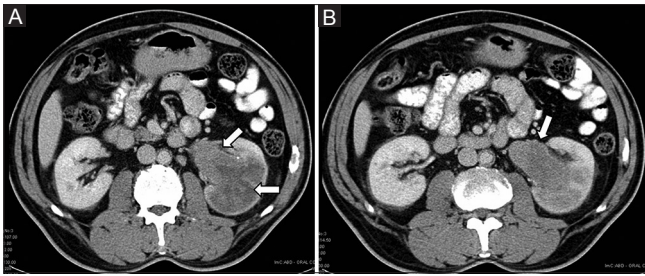


**Figure 26:** (A, B) Infiltrative TCC: Axial contrast-enhanced CT images showing mildly enhancing bean-type renal mass involving the collecting system extending into the renal pelvis of left kidney (arrows)

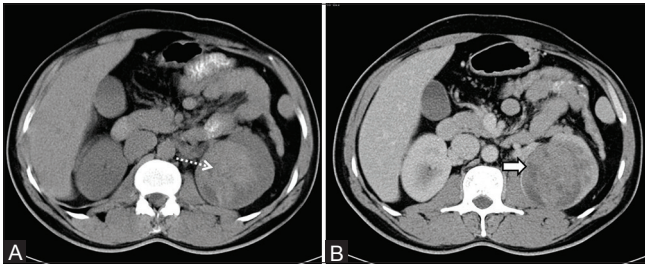


**Figure 28 (A and B):** (A, B): Extrasosseous Ewing's sarcoma: (A) Unenhanced CT image showing expansive left renal mass with hyperdense contents suggestive of hemorrhage (B) contrast-enhanced CT image showing mild heterogeneous enhancement of the lesion with necrosis histopathologically proven to be extrasosseous Ewing's sarcoma of kidney in a 36-year-old-male

benign renal tissue, and are therefore referred to as renal pseudotumors. Pseudotumors can be developmental (prominent columns of Bertin, persistent fetal lobulation, dromedary hump, splenorenal fusion, cross-fused renal ectopia), infectious (abscess, pyelonephritis, scarred kidney), granulomatous, vascular (extramedullary hematopoiesis, arteriovenous malformation, hematoma), and regenerating nodules post reflux [Figures 32 and 33].<sup>[70]</sup>

### Current Role of Renal Biopsy

At present, percutaneous pretreatment biopsy to identify benign vs. malignant in small solid renal masses (<4cm) is said to be reliable and cost effective.<sup>[71,72]</sup> Long-held concerns preventing the incorporation of biopsies into routine patient care, including the perception of poor diagnostic yield and risks of complications such as bleeding or biopsy tract seeding, have largely been disproven.<sup>[73]</sup> A recent meta-analysis of 5228 biopsies identified less than 1% of patients with complications.<sup>[71]</sup> As more patients with renal masses are treated with thermal ablation,<sup>[74]</sup> establishing an upfront cancer diagnosis from renal tumor biopsy is exceptionally important. Biopsy should be performed before the day of treatment so that patients can use the biopsy findings to help make an informed decision prior to treatment. However, one should be aware of biopsy limitations. Pathology from renal mass biopsy may underestimate the nuclear grade or fail to identify aggressive pathologic features in renal cell cancer because

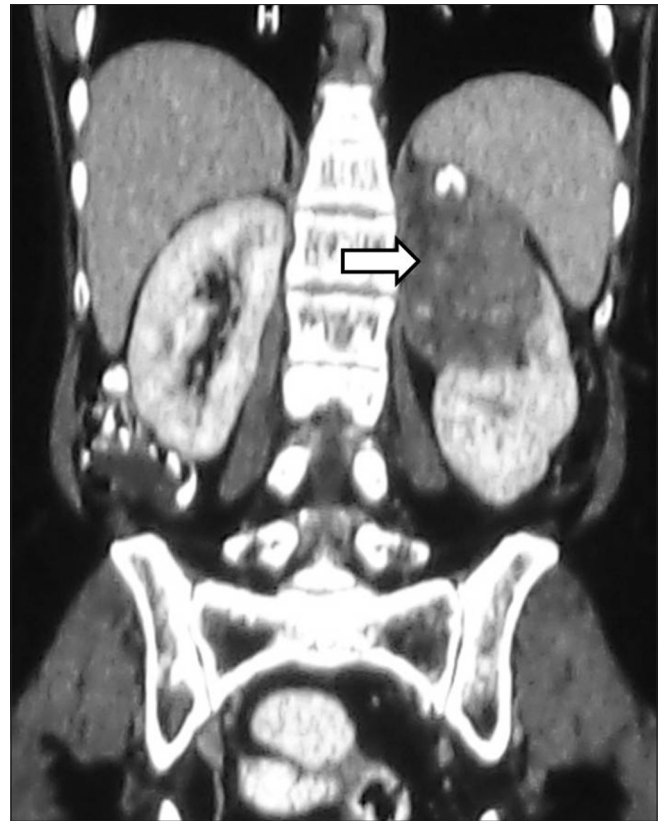


**Figure 27:** Mesenchymal tumor: Coronal contrast-enhanced CT image showing ball-type renal mass (arrow) in left kidney with calcification histopathologically proven to be mesenchymal renal mass

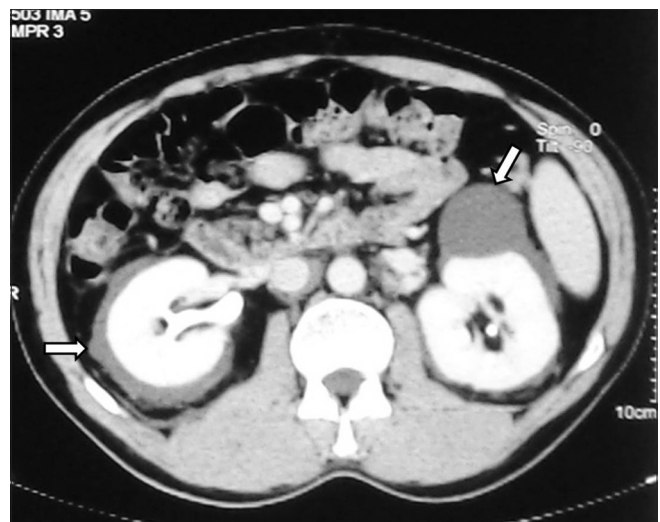


**Figure 29:** Renal lymphangiectasia: Axial contrast-enhanced CT image showing cystic attenuation lesion in bilateral perinephric space suggestive of lymphangiectasia

of sampling error in heterogeneous tumors. At present, renal biopsy from small solid renal masses may be useful as patients and physicians can use information from biopsy to make more informed decisions among treatments, and the routine use of biopsy decreases overtreatment of incidentally detected benign tumors.<sup>[75]</sup>

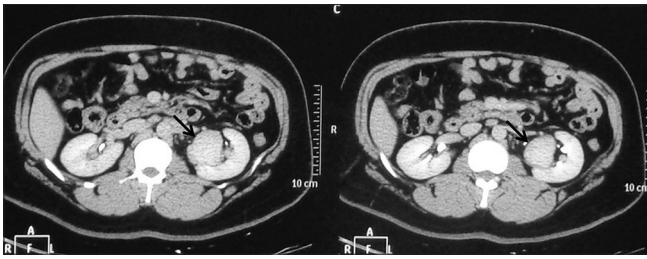


**Figure 30:** Renal hemangioma: Axial contrast-enhanced CT image showing intensely enhancing mass (arrow) in left kidney confirmed to be a case of renal hemangioma

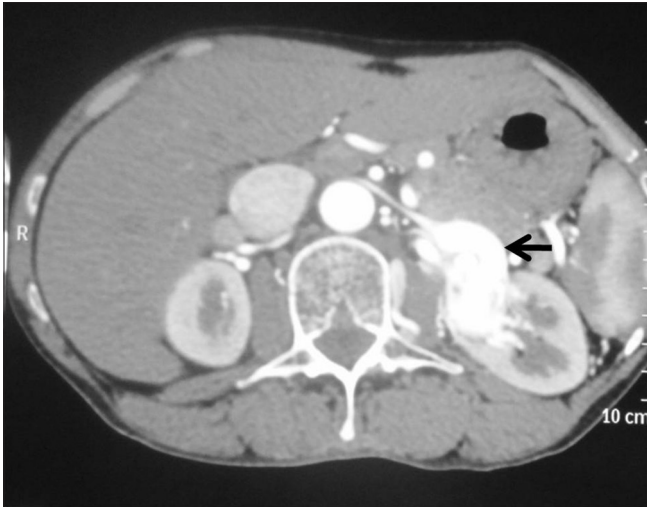


**Figure 32:** Renal artery aneurysm: Axial contrast-enhanced CT image showing intensely enhancing left renal artery aneurysm (arrow)

### Challenges in Diagnosis of Small Renal Masses

Most small renal masses are benign cysts but some are solid and/or cystic that can range from benign AMLs, adenomas, and oncocytomas to RCC. Of the small solid renal masses, only fat-containing AML can be confidently diagnosed. Solid renal masses especially less than 1.5 cm in diameter can be problematic and challenging due to varied imaging spectrum of various benign and malignant masses depending on the composition of the renal tumor. Interdepartmental, clinical, and use of multimodality imaging sometimes can be helpful in difficult cases. Observation or watchful waiting is generally recommended for masses that are probably benign; a low probability of malignancy exists, hence, the mass can be observed with serial imaging.

### Conclusion

It is not easy to differentiate small renal masses into benign vs. malignant when the imaging is not classical. Multidisciplinary approach is required which comes from experience and learning. The key teaching points of our

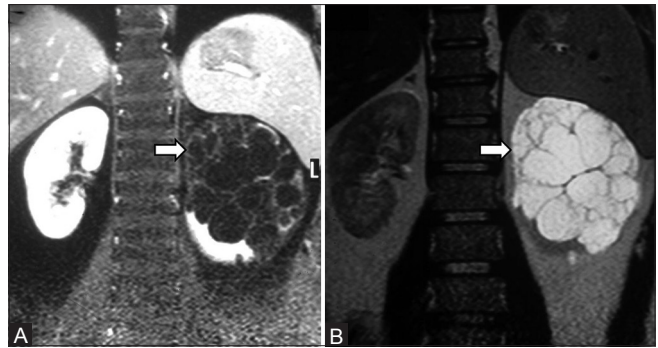


**Figure 31 (A and B):** (A, B): Cystic nephroma: Coronal T1 and T2-weighted MR images showing multicystic lesion in left kidney with thin septations proven to be cystic nephroma



**Figure 33:** Arteriovenous malformation: Coronal contrast-enhanced CT image showing arteriovenous malformation (arrow) in the left perinephric and pararenal space

experience has been highlighted in Table 4. Identifying enhancement in small renal masses is of utmost importance and should be differentiated from pseudoenhancement. Furthermore, characterization of renal masses into benign, borderline, and malignant nature at an early stage can change the management and outcome. Small renal masses sized less than 2 cm are usually benign and if imaging features are indeterminate then depending upon the clinical presentation and demographic data, observation with serial imaging or percutaneous biopsy can be done.

### Acknowledgement

IRIA for the Dr. N. G. Gadekar Memorial Oration Award 2016.

**Table 4: Key teaching points**

True enhancement and pseudoenhancement must be identified  
 Enhancement is said to be significant if it is greater than 15 HU  
 Enhancement between 10-15HU is indeterminate.  
 Four-phase CECT is the imaging modality of choice for renal mass characterization  
 Renal masses <4cm in diameter are small renal masses and are likely to be benign  
 Solid renal tumors are divided into pseudotumors, typical AML, indeterminate lesion, and typical RCC  
 Central necrosis and calcification is suggestive of RCC  
 Fat, necrosis, and calcification may be suggestive of RCC with fatty component  
 Homogeneous enhancement, scar, and segmental enhancement inversion is in favour of oncocytoma  
 Lipid poor AML cannot be differentiated from RCC on imaging  
 Lipid poor AML is hyperattenuating (>45 HU) on unenhanced CT, and hypointense on T1 and T2-weighted MRI  
 Hemangioma and osteosarcoma should be considered as a differential when a calcified renal mass is encountered  
 Fat containing renal masses are AML, lipoma, and fat containing RCC  
 Renal masses with epicentre in the medullary region are AML, medullary fibroma, hemangioma, renal medullary carcinoma, and carcinoma of collecting duct of Bellini  
 Solid, homogeneous mass centered in the collecting system extending into the ureteropelvic junction is more likely to be an intrarenal TCC  
 Small RCCs may not show enhancement and may be misinterpreted as a hyperattenuating cyst. Most RCCs below these enhancement thresholds are papillary RCC  
 Renal masses with borderline enhancement on CT should be further evaluated with MRI or contrast-enhanced ultrasound

**Financial support and sponsorship**

Nil.

**Conflicts of interest**

There are no conflicts of interest.

**References**

- Jemal A, Siegel R, Xu J, Ward E. Cancer statistics, 2010. *CA Cancer J* 2010;60:277-300.
- Agnihotri S, Kumar J, Jain M, Kapoor R, Mandhani A. Renal cell carcinoma in India demonstrates early age of onset and a late stage of presentation. *Indian J Med Res* 2014;140:624-9.
- Kovacs G, Akhtar M, Beckwith BJ, Bugert P, Cooper CS, Delahunt B, *et al.* The Heidelberg classification of renal cell tumours. *J Pathol* 1997;183:131-3.
- Pahernik S, Ziegler S, Roos F, Melchior SW, Thüroff JW. Small renal tumors: Correlation of clinical and pathological features with tumor size. *J Urol* 2007;178:414-7.
- Gerst S, Hann LE, Li D, Gonen M, Tickoo S, Sohn MJ, *et al.* Evaluation of renal masses with contrast-enhanced ultrasound: Initial experience. *AJR Am J Roentgenol* 2011;197:897-906.
- Xu ZF, Xu HX, Xie XY, Liu GJ, Zheng YL, Lu MD. Renal cell carcinoma and renal angiomyolipoma: Differential diagnosis with real-time contrast-enhanced ultrasonography. *J Ultrasound Med* 2010;29:709-17.
- Cokkinos DD, Antypa EG, Skilakaki M, Kriketou D, Tavernaraki E, Piperopoulos PN. Contrast enhanced ultrasound of the kidneys: What is it capable of? *Biomed Res Int* 2013;2013:595873.
- Montravers F, Grahek D, Kerrou K, Younsi N, Doublet JD, Gattegno B, *et al.* Evaluation of FDG uptake by renal malignancies (primary tumor or metastases) using a coincidence detection gamma camera. *J Nucl Med* 2000;41:78-84.
- Hélénon O, Eiss D, Debrito P, Merran S, Correas JM. How to characterise a solid renal mass: A new classification proposal for a simplified approach. *Diagn Interv Imaging* 2012;93:232-45.
- Mileto A, Nelson RC, Paulson EK, Marin D. Dual-Energy MDCT for Imaging the Renal Mass. *AJR Am J Roentgenol* 2015;204:W640-7.
- Kaza RK, Platt JF. Renal applications of dual-energy CT. *Abdom Radiol* 2016;41:1122-32.
- Mileto A, Marin D, Ramirez-Giraldo JC, Scribano E, Krauss B, Mazziotti S, *et al.* Accuracy of contrast-enhanced dual-energy MDCT for the assessment of iodine uptake in renal lesions. *AJR Am J Roentgenol.* 2014;202:W466-74.
- Mileto A, Marin D, Alfaro-Cordoba M, Ramirez-Giraldo JC, Eusemann CD, Scribano E, *et al.* Iodine quantification to distinguish clear cell from papillary renal cell carcinoma at dual-energy multidetector CT: A multireader diagnostic performance study. *Radiology* 2014;273:813-20.
- Pedrosa I, Sun MR, Spencer M, Genega EM, Olumi AF, Dewolf WC, *et al.* MR imaging of renal masses: Correlation with findings at surgery and pathologic analysis. *Radiographics* 2008;28:985-1003.
- Mirka H, Korcakova E, Kastner J, Hora M, Hes O, Hosek P, *et al.* Diffusion-weighted imaging using 3.0 T MRI as a possible biomarker of renal tumors. *Anticancer Res* 2015;35:2351-7.
- Dyer R, DiSantis DJ, McClennan BL. Simplified imaging approach for evaluation of the solid renal mass in adults. *Radiology* 2008;247:331-43.
- Hartman DS, Davidson AJ, Davis CJ Jr, Goldman SM. Infiltrative renal lesions: CT sonographic-pathologic correlation. *AJR Am J Roentgenol* 1988;150:1061-4.
- Pickhardt PJ, Lonergan GJ, Davis CJ Jr, Kashitani N, Wagner BJ. Infiltrative renal lesions: Radiologic-pathologic correlation. *Radiographics* 2000;20:215-43.
- Ng CS, Wood CG, Silverman PM, Tannir NM, Tamboli P, Sandler CM. Renal cell carcinoma: Diagnosis, staging, and surveillance. *AJR Am J Roentgenol* 2008;191:1220-32.
- Jemal A, Siegel R, Ward E, Murray T, Xu J, Thun MJ. Cancer statistics, 2007. *CA Cancer J Clin* 2007;57:43-66.
- Eble JN, Sauter G, Epstein JI, Sesterhenn IA, editors. World Health Organization classification of tumours: Pathology and genetics of tumours of the urinary system and male genital organs. Lyon, France: IARC; 2004.
- Grignon DJ, Che M. Clear cell renal cell carcinoma. *Clin Lab Med* 2005;25:305-16.
- Lopez-Beltran A, Scarpelli M, Montironi R, Kirkali Z. 2004 WHO classification of the renal tumors of the adults. *Eur Urol* 2006;49:798-805.
- Outwater EK, Bhatia M, Siegelman ES, Burke MA, Mitchell DG. Lipid in renal clear cell carcinoma: Detection on opposed-phase gradient-echo MR images. *Radiology* 1997;205:103-7.
- Herts BR, Coll DM, Novick AC, Obuchowski N, Linnell G, Wirth SL, *et al.* Enhancement characteristics of papillary renal neoplasms revealed on triphasic helical CT of the kidneys. *AJR Am J Roentgenol* 2002;178:367-72.
- Kim JK, Kim TK, Ahn HJ, Kim CS, Kim KR, Cho KS. Differentiation of subtypes of renal cell carcinoma on helical CT scans. *AJR Am J Roentgenol* 2002;178:1499-506.
- Raman SP, Johnson PT, Allaf ME, Netto G, Fishman EK. Chromophobe renal cell carcinoma: Multiphase MDCT enhancement patterns and morphologic features. *AJR Am J Roentgenol* 2013;201:1268-76.
- Hu Y, Lu GM, Li K, Zhang LJ, Zhu H. Collecting duct carcinoma

- of the kidney: Imaging observations of a rare tumor. *Oncol Lett* 2014;7:519-24.
29. Alappan N, Marak CP, Chopra A, Joy PS, Dorokhova O, Guddati AK. Renal medullary cancer in a patient with sickle cell trait. *Case Rep Oncol Med* 2013;2013:129813.
  30. Blitman NM, Berkenblit RG, Rozenblit AM, Levin TL. Renal medullary carcinoma: CT and MRI features. *AJR Am J Roentgenol* 2005;185:268-72.
  31. Woo S, Kim SY, Lee MS, Moon KC, Kim SH, Cho JY, *et al.* MDCT findings of renal cell carcinoma associated with Xp11.2 translocation and TFE3 gene fusion and papillary renal cell carcinoma. *AJR Am J Roentgenol* 2015;204:542-9.
  32. Sureka B, Bansal K, Arora A. Imaging hallmark of Xp11.2 translocation renal cell carcinoma. *Can Urol Assoc J* 2015;9:E572.
  33. Morna Palmeiro M, Niza JL, Loureiro AL, Conceição E Silva JP. Unusual renal tumour: Multilocular cystic renal cell carcinoma. *BMJ Case Rep* 2016pii: Bcr2016214386.
  34. Chao DH, Zisman A, Pantuck AJ, Freedland SJ, Said JW, Belldegrun AS. Changing concepts in the management of renal oncocytoma. *Urology* 2002;59:635-42.
  35. Ishigami K, Jones AR, Dahmouh L, Leite LV, Pakalniskis MG, Barloon TJ. Imaging spectrum of renal oncocytomas: A pictorial review with pathologic correlation. *Insights Imaging* 2015;6:53-64.
  36. Kim JI, Cho JY, Moon KC, Lee HJ, Kim SH. Segmental enhancement inversion at biphasic multidetector CT: Characteristic finding of small renal oncocytoma. *Radiology* 2009;252:441-8.
  37. McGahan JP, Lamba R, Fisher J, Starshak P, Ramsamooj R, Fitzgerald E, *et al.* Is segmental enhancement inversion on enhanced biphasic MDCT a reliable sign for the noninvasive diagnosis of renal oncocytomas? *AJR Am J Roentgenol* 2011;197:W674-9.
  38. Kodama K, Nagano K, Akimoto M, Suzuki S. Small renal oncocytoma with central cystic degeneration. *Int J Urol* 2004;11:110-3.
  39. Xiao GQ, Ko HB, Unger P. Telangiectatic oncocytoma: A previously undescribed variant of renal oncocytoma. *Am J Clin Pathol* 2013;140:103-8.
  40. Dechet CB, Bostwick DG, Blute ML, Bryant SC, Zincke H. Renal oncocytoma: Multifocality, bilateralism, metachronous tumor development and coexistent renal cell carcinoma. *J Urol* 1999;162:40-2.
  41. Rowsell C, Fleshner N, Marrano P, Squire J, Evans A. Papillary renal cell carcinoma within a renal oncocytoma: Case report of an incidental finding of a tumour within a tumour. *J Clin Pathol* 2007;60:426-8.
  42. Noguchi S, Nagashima Y, Shuin T, Kubota Y, Kitamura H, Yao M, *et al.* Renal oncocytoma containing "chromophobe" cells. *Int J Urol* 1995;2:279-80.
  43. Ball DS, Friedman AC, Hartman DS, Radecki PD, Caroline DF. Scar sign of renal oncocytoma: Magnetic resonance imaging appearance and lack of specificity. *Urol Radiol* 1986;8:46-8.
  44. Sun J, Xing Z, Xing W, Zheng L, Chen J, Fan M, *et al.* Intratumoral Macroscopic Fat and Hemorrhage Combination Useful in the Differentiation of Benign and Malignant Solid Renal Masses. *Medicine* 2016;95:e2960.
  45. Davarpanah AH, Spektor M, Mathur M, Israel GM. Homogeneous T1 Hyperintense Renal Lesions with Smooth Borders: Is Contrast-enhanced MR Imaging Needed? *Radiology* 2016;280:128-36.
  46. Olusanya AA, Huff G, Adeleye O, Faulkner M, Burnette R, Thompson H, *et al.* Primary renal non-Hodgkins lymphoma presenting with acute renal failure. *J Natl Med Assoc* 2003;95:220-4.
  47. Malbrain ML, Lambrecht GL, Daelemans R, Lins RL, Hermans P, Zachee P. Acute renal failure due to bilateral lymphomatous infiltrates: Primary extranodal non-Hodgkin's lymphoma (p-EN-NHL) of the kidneys—Does it really exist? *Clin Nephrol* 1994;42:163-9.
  48. Sheth S, Ali S, Fishman E. Imaging of renal lymphoma: Patterns of disease with pathologic correlation. *Radiographics* 2006;26:1151-68.
  49. Ganeshan D, Iyer R, Devine C, Bhosale P, Paulson E. Imaging of primary and secondary renal lymphoma. *AJR Am J Roentgenol* 2013;201:W712-9.
  50. Jinzaki M, Silverman SG, Akita H, Nagashima Y, Mikami S, Oya M. Renal angiomyolipoma: A radiological classification and update on recent developments in diagnosis and management. *Abdom Imaging* 2014;39:588-604.
  51. Lane BR, Aydin H, Danforth TL, Zhou M, Remer EM, Novick AC, *et al.* Clinical correlates of renal angiomyolipoma subtypes in 209 patients: Classic, fat poor, tuberous sclerosis associated and epithelioid. *J Urol* 2008;180:836-43.
  52. Siegel CL, Middleton WD, Teefey SA, McClennan BL. Angiomyolipoma and renal cell carcinoma: US differentiation. *Radiology* 1996;198:789-93.
  53. Jinzaki M, Ohkuma K, Tanimoto A, Mukai M, Hiramatsu K, Murai M, *et al.* Small solid renal lesions: Usefulness of power Doppler US. *Radiology* 1998;209:543-50.
  54. Ellingson JJ, Coakley FV, Joe BN, Qayyum A, Westphalen AC, Yeh BM. Computed tomographic distinction of perirenal liposarcoma from exophytic angiomyolipoma: A feature analysis study. *J Comput Assist Tomogr* 2008;32:548-52.
  55. Jinzaki M, Tanimoto A, Narimatsu Y, Ohkuma K, Kurata T, Shinmoto H, *et al.* Angiomyolipoma: Imaging findings in lesions with minimal fat. *Radiology* 1997;205:497-502.
  56. Mikami S, Oya M, Mukai M. Angiomyolipoma with epithelial cysts of the kidney in a man. *Pathol Int* 2008;58:664-7.
  57. Froemming AT, Boland J, Cheville J, Takahashi N, Kawashima A. Renal epithelioid angiomyolipoma: Imaging characteristics in nine cases with radiologic-pathologic correlation and review of the literature. *AJR Am J Roentgenol* 2013;200:W178-86.
  58. Tsukada J, Jinzaki M, Yao M, Nagashima Y, Mikami S, Yashiro H, *et al.* Epithelioid angiomyolipoma of the kidney: Radiological imaging. *Int J Urol* 2013;20:1105-11.
  59. Crino PB, Nathanson KL, Henske EP. The tuberous sclerosis complex. *N Engl J Med* 2006;355:1345-56.
  60. Johnson SR, Cordier JF, Lazor R, Cottin V, Costabel U, Harari S, *et al.* European Respiratory Society guidelines for the diagnosis and management of lymphangioleiomyomatosis. *Eur Respir J* 2010;35:14-26.
  61. Akasbi Y, Arifi S, Lahlaidi K, Namad T, Mellas N, El Fassi MJ, *et al.* Renal metastases of a femur osteosarcoma: A case report and a review of the literature. *Case Rep Urol* 2012;2012:259193.
  62. Choyke PL, White EM, Zeman RK, Jaffe MH, Clark LR. Renal metastases: Clinicopathologic and radiologic correlation. *Radiology* 1987;162:359-63.
  63. Rayer PF. *Traité des maladies du reins*. vol. 3. Paris, France: JB Baillier; 1841. p. 699.
  64. Rathmell WK, Godley PA. Recent updates in renal cell carcinoma. *Curr Opin Oncol* 2010; 22: 250-6.
  65. Raza SA, Sohaib SA, Sahdev A, Bharwani N, Heenan S, Verma H, *et al.* Centrally infiltrating renal masses on CT: Differentiating intrarenal transitional cell carcinoma from centrally located renal cell carcinoma. *AJR Am J Roentgenol* 2012;198:846-53.
  66. Caoili EM, Cohan RH, Inampudi P, Ellis JH, Shah RB, Faerber GJ, *et al.* MDCT urography of upper tract urothelial neoplasms. *AJR Am J Roentgenol* 2005;184:1873-81.
  67. Katabathina VS, Vikram R, Nagar AM, Tamboli P, Menias CO, Prasad SR. Mesenchymal neoplasms of the kidney in adults: Imaging spectrum with radiologic-pathologic correlation. *Radiographics* 2010;30:1525-40.

68. Wilkinson C, Palit V, Bardapure M, Thomas J, Browning AJ, Gill K, *et al.* Adult multilocular cystic nephroma: Report of six cases with clinical, radio-pathologic correlation and review of literature. *Urol Ann* 2013;5:13-7.
69. Brown RC, Cornell SH, Culp DA. Multilocular renal cyst with diffuse calcification simulating renal cell carcinoma. *Radiology* 1970;95:411-2.
70. Bhatt S, MacLennan G, Dogra V. Renal pseudotumors. *AJR Am J Roentgenol* 2007;188:1380-7.
71. Marconi L, Dabestani S, Lam TB, Hofmann F, Stewart F, Norrie J, *et al.* Systematic Review and Meta-analysis of Diagnostic Accuracy of Percutaneous Renal Tumour Biopsy. *Eur Urol* 2016;69:660-73.
72. Heilbrun ME, Yu J, Smith KJ, Dechet CB, Zagoria RJ, Roberts MS. The cost-effectiveness of immediate treatment, percutaneous biopsy and active surveillance for the diagnosis of the small solid renal mass: Evidence from a Markov model. *J Urol* 2012;187:39-43.
73. Evans AJ, Delahunt B, Srigley JR. Issues and challenges associated with classifying neoplasms in percutaneous needle biopsies of incidentally found small renal masses. *Semin Diagn Pathol* 2015;32:184-95.
74. Choueiri TK, Schutz FA, Hevelone ND, Nguyen PL, Lipsitz SR, Williams SB, *et al.* Thermal ablation vs surgery for localized kidney cancer: A Surveillance, Epidemiology, and End Results (SEER) database analysis. *Urology* 2011;78:93-8.
75. Jason Abel E. Percutaneous biopsy facilitates modern treatment of renal masses. *Abdom Radiol* 2016;41:617-9.